Petroleum Science 21 (2024) 823–835

Contents lists available at ScienceDirect

Petroleum Science

journal homepage: www.keaipublishing.com/en/journals/petroleum-science

Original Paper

Stratigraphic framework and sedimentary evolution during the Cryogenian-Ediacaran transition in northeastern Sichuan Basin, South China

Yi Zhang [a, b, c, 1], Hong-Wei Kuang [a, 1], Yong-Qing Liu [a], Qiang Shi [c], Dong-Ge Wang [c], Ke-Ning Qi [a], Yu-Chong Wang [a], Da-Wei Qiao [a], Xiao-Shuai Chen [a], Li-Zhi Wu [c], Meng Tian [c], Long Chen [c], Yi Wei [c], Liao-Yuan Song [c], Jian Li [c], Zi-Gang Wu [b], Yun-Qian Liu [b], Xuan-Chun Liu [d], An-Qing Chen [e], Zhi-Wei Liao [b, *]

[a] Institute of Geology, Chinese Academy of Geological Sciences, Beijing, 100037, China
[b] State Key Laboratory of Coal Mine Disaster Dynamics and Control, School of Resources and Safety Engineering, Chongqing University, Chongqing, 400044, China
[c] No. 205 Geological Team, Chongqing Bureau of Geology and Minerals Exploration, Chongqing, 401121, China
[d] Chongqing Institute of Geological Survey, Chongqing, 401122, China
[e] Key Laboratory of Deep-time Geography and Environment Reconstruction and Applications of Ministry of Natural Resources, Chengdu University of Technology, Chengdu, 610059, Sichuan, China

ARTICLE INFO

Article history:
Received 29 December 2022
Received in revised form
16 August 2023
Accepted 13 December 2023
Available online 22 December 2023

Edited by Jie Hao

Keywords:
Marinoan glaciation
Doushantuo formation
Cap dolomite
Deglacial and coastal deposits
Detrital zircon U-Pb dating

ABSTRACT

The northeastern Sichuan area in the northern Yangtze margin has unique Ediacaran geological records, especially the Doushantuo Formation (DST), and become a hot research area in recent years. However, the Cryogenian-Ediacaran (C-E) boundary has not been precisely identified, which restricts the in-depth study of geological information during this crucial transitional period and is unfavorable for a systematic and complete understanding of the Yangtze Block and even the global paleogeographic pattern. This study conducted stratigraphy, sedimentology, and chronostratigraphy to establish the stratigraphic framework and sedimentary evolution of the C-E transition strata in northeastern Sichuan. The results showed that the Ediacaran sediments, without the cap dolomite, unconformably overlaid the Cryogenian sediments in the studied area. The Member II of the DST, characterized by 50–160 m of red-green sandstone (approximately equivalent to the original Chengkou "Guanyinya Formation"), directly overlaid the Cryogenian sediments and displayed a 623 ± 2.3 Ma maximum depositional age from the detrital zircon U–Pb dating. Regional stratigraphic correlations indicate that the C-E transition strata in northeastern Sichuan had a consistent lithological association and sedimentary sequence characteristics but differed from the Three Gorges. Typically, the upper Nantuo massive glacial diamictites transition to the icebergs rafted lonestone-bearing mudstones at the top, then change upward to DST barrier coast sandstones. The proposed DST of the northeastern Sichuan Basin was divided into three lithostratigraphic members without the regional Member I cap dolomite: (i) Member II purple-red, gray-green sandstone strata, (ii) Member III black mudstone strata, and (iii) Member IV P–Mn bearing strata. During the C-E transition, the study area experienced (i) the global deglaciation stage in the terminal Marinoan glaciation and (ii) the filling-leveling up stage with clastic rocks in the early Ediacaran. Overall, the early Ediacaran of northeastern Sichuan succeeded the paleogeographic features of the late Cryogenian.

1. Introduction

Due to the progressive success of the Ediacaran oil-gas exploration and development in South China, such as the Anyue Gas Field in the Sichuan Basin and Doushantuo shale gas in Three Gorges (Liu

* Corresponding author.
E-mail address: zwliao16@cqu.edu.cn (Z.-W. Liao).
[1] Y. Zhang and H. W. Kuang contributed equally to this paper.

https://doi.org/10.1016/j.petsci.2023.12.011

et al., 2019; Wang et al., 2019), the Ediacaran Doushantuo Formation (DST) has been a focus of source rock evaluation. In recent years, northeastern Sichuan has been a popular research area as the DST records (i) extremely high organic matter enrichment and widespread effective hydrocarbon source rocks with a large thickness (Xiao et al., 2020a; Zhu et al., 2022), (ii) depositional events of large-scale phosphorite and manganese (Zhang et al., 2021), and (iii) rare micropaleontology records of the latest DST period (Zhang, 2014). It indicates considerable potential for hydrocarbon exploration in the region. These unique geological records also provide a new opportunity to decipher major geological events and understand the Earth's evolution during this critical geological period. However, the stratigraphic framework in northeastern Sichuan is limited to controversially macroscopic lithostratigraphy, restricting the in-depth study.

In South China, the DST (635–535 Ma) is typically divided into four members (Jiang et al., 2011): (i) Member I (DST I), the Marinoan cap dolomite; (ii) Member II (DST II), the lower shales; (iii) Member III (DST III), the upper dolomites; (iv) Member IV (DST IV), the upper shales. In the northeastern Sichuan Basin, the DST is commonly regarded as a black rock strata, rich in organic matter and bearing phosphorus and manganese in the upper regions (Wang et al., 2020a; Xiao et al., 2020a). The red and green clastic rock strata (Chengkou Guanyinya Formation), between the Cryogenian Nantuo glacial diamictites and Ediacaran Doushantuo black rock strata, remains unclear in its identification as either Cryogenian or Ediacaran. There are five proposals for its stratigraphic division and correlation in the study area as (Fig. S1): (i) an individual formation (Guanyinya Formation), belonging to the early Ediacaran (Li and Zhou, 1995) or (ii) late Cryogenian (Zhang, 2015); (iii) the top strata of the Cryogenian Nantuo Formation (NT) (Li et al., 2019); (iv) the DST lower strata (Zhang et al., 2021); or with (v) the lower region assigned to the NT and the upper region assigned to the DST (Wang et al., 2021b). Moreover, there is a set of lonestone-bearing mudstones (10–20 m) overlying the NT glacial diamictites, which have not been previously studied.

The Guanyinya Formation is typically developed in western Sichuan with a thickness of 100–150 m, equivalent to the DST as contemporaneous difference facies, and features clastic rock strata in the lower part, dolomite strata in the middle part, and limestone strata in the upper part (Zhou et al., 2021). Due to the lack of chronostratigraphy, chemostratigraphy, biostratigraphy, and sedimentology studies, the bottom DST boundary in northeastern Sichuan has not been precisely defined. Determining or clarifying the age and attribution of the Guanyinya Formation has become essential to establish the stratigraphic framework in the northeastern Sichuan accurately. Moreover, the existence of cap dolomite at the bottom of the DST is still widely controversial (Wang et al., 2019, 2020a; Xiao et al., 2020). Therefore, the uncertainty or controversy surrounding the Cryogenian-Ediacaran (C-E) boundary in northeastern Sichuan has severely restricted the understanding of the biological evolution, paleogeography, and paleoenvironment during this period; thus, further making it unfavorable for the in-depth study of the Ediacaran oil-gas system. Based on six new outcrops and well drillings, we reconstructed the stratigraphic framework of the C-E transition strata in northeastern Sichuan through detailed sedimentological and stratigraphical analysis and detrital zircon geochronology. This study will provide new materials and evidence to improve the paleogeographic pattern of the C-E transition in the study area.

2. Geological setting

The study area is located in the Zhenba-Chengkou-Wuxi region, on the northern Yangtze Margin, adjacent to the south Qinling orogen in the north and borders the Sichuan Basin in the south (Fig. 1). The C-E strata in the study area comprises of a thick sedimentary record beginning with the opening of the Neoproterozoic Nanhua Rift. The stratigraphy comprises the Tonian Longtanhe Formation, Cryogenian Daianhe and Nantuo formations, and Ediacaran Doushantuo and Dengying formations, in ascending order. In the Chengkou region, the Longtanhe Formation is a rift-filling sequence of volcanic clastic rocks thicker than 2000 m, with an age of 777 Ma provided by volcanic ash beds near the top of the succession (Xiang et al., 2015). The Daianhe and Nantuo formations are approximately 490 m and 1560 m thick (Li et al., 2021b), respectively, and the latter is interpreted as younger than 639 Ma (Huang et al., 2021). These units are dominated by glacial diamictites of rift sequences and record two Cryogenian glacial events. The Ediacaran is mainly characterized by the carbonate platform-building sequence, which changes from the lower clastic rock strata to the upper DST black rock strata (ca. 90–200 m, Zhang et al., 2021). Then, it is transformed into a giant thickness (ca. 105–900 m) of Dengying carbonate rocks and microbialites (Li et al., 2019).

During the Cryogenian, the study area was located in the Central Nanhua Rift Basin on the northern Yangtze Margin. The filling features and gravity anomaly data indicate that this rift extends east-west from northeastern Sichuan to the Wudang uplift (Li et al., 2021b) and probably connects with the contemporaneous central Sichuan rift (Xiao et al., 2020). Seismic profiles and stratigraphic features indicate that both the Nanhua rifts in the northern Yangtze Margin and central Sichuan were filled before the Ediacaran deposition (Xiao et al., 2020). In the early Ediacaran, the sedimentary strata of the study area were influenced by the eroded landform of the Marinoan Glaciation (Xiao et al., 2020). In the late Ediacaran, intracratonic rifts developed in the northern Yangtze Block, such as the Mianyang-Changning, Wanyuan-Dazhou, and West Hubei-East Chongqing Rifts (Li et al., 2019; Wang et al., 2021b).

3. Materials and methods

Along the Chengkou-Fangxian fault, seven outcrops and two well drillings for the C-E transition strata were measured and logged on a scale of 1:200. The detailed lithology and sedimentary structures were described in the field. In the Lijiagou section, we collected 25 samples targeting the C-E transition stratigraphy for thin section analysis. One sandstone sample (ZK117-1-49) was collected at ZK117-1 for detrital zircon U–Pb dating, and one phosphorite sample from ZK0-11 was collected for microfossil analysis. Petrographical studies were conducted on thin sections in transmitted light by a Zeiss Scope A1 polarizing microscope. For the detrital zircons, the separate, select, target preparation, cathodoluminescence photo, and U–Pb dating analyses were conducted at the Beijing CreaTech Testing Technology Co., Ltd. U–Pb dating analyses were conducted using a laser inductively coupled plasma mass spectrometer, with analytical conditions and approaches in reference to Hou et al. (2009) and Wang et al. (2021a). Off-line raw data selection and integration of background and analyte signals, as well as time-drift correction and quantitative

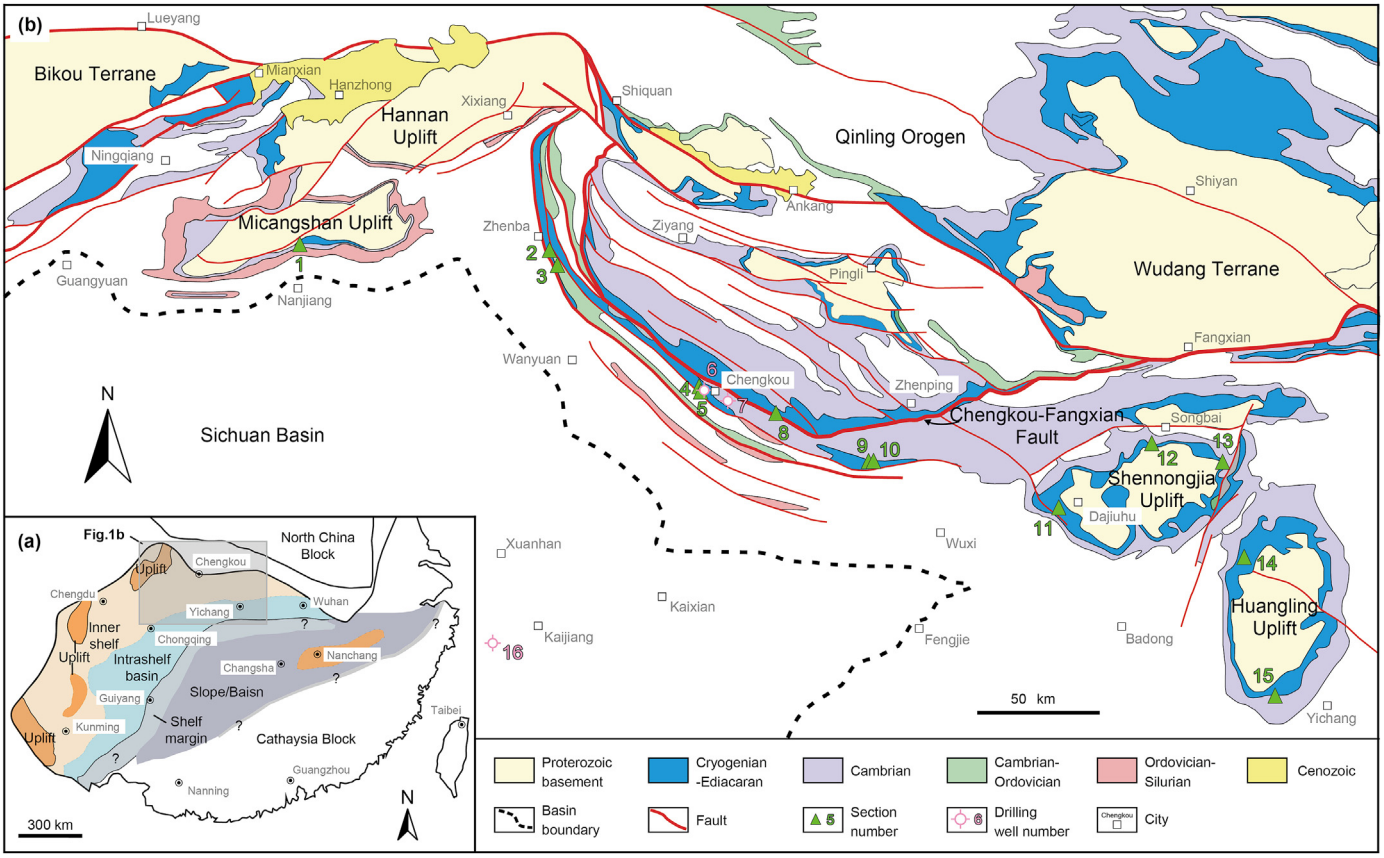

Fig. 1. Location map of the study area. **(a)** Palaeogeographic map of the Yangtze Block during the Ediacaran Doushantuo period (modified from Jiang et al., 2011; Wang et al., 2019); **(b)** Simplified geological map of the northeastern Sichuan Basin (modified from Wang et al., 2020a). Section or well number: 1: Yangba, Nanjiang (Wang et al., 2019); 2: Xiaoyangba, Zhenba; 3: Lianghekou, Zhenba; 4: Caojiashan, Chengkou; 5: Lijiagou, Chengkou; 6: ZK117-1, Chengkou; 7: ZK0-11, Chengkou; 8: Heyu, South Qinling, Chengkou; 9: Longjiapo, Wuxi; 10: Gaozu, Wuxi; 11: Gaoqiaohe-Guogongping, Shennongjia (Kuang et al., 2022); 12: Mahuanggou, Shennongjia (Kuang et al., 2022); 13: Lianhua, Shennongjia (Ye et al., 2022); 14: Gaolan, Xingshan (Chen et al., 2023); 15: Jiulongwan, Yichang (Jiang et al., 2011); 16: WT-1, Kaijiang (He et al., 2021).

calibration for U–Pb dating, were performed using LADR_1.1.07. (Norris and Danyushevsky, 2018). The common Pb correction was unnecessary in all analyzed zircon grains due to the low signal of common ^{204}Pb and high $^{206}Pb/^{204}Pb$. Concordia diagrams and weighted mean calculations were made using Isoplot software (Ludwig, 2003).

4. Results

4.1. Sedimentary characteristics

Along the NW-SE profile of the C-E transition strata in the northeastern Sichuan Basin, consistent stratigraphic features and sequences were observed (Fig. 2; see detailed description in Supplementary Material). In terms of stratigraphy, the lower transition strata were NT diamictites, consisting of 65–95% arenaceous and clayey matrix and 5–35% polymictic gravels dominated by granite, sandstone, and mafic igneous rocks (Fig. 3(a) and S2(a)). Gravels were mainly angular, poorly sorted, and 0.2–50 cm in size. Diamictite was massive and developed a lamination (Fig. 3(a) and S2(a)).

The middle transition strata comprised lenticular pebbly sandstones (Fig. 3(b) and S2(d)–(g)), massive lonestone-bearing siltstones (Fig. S6(a)), and laminated lonestone-bearing mudstones (Fig. 3(c)–(e)). The pebbly sandstone consisted of medium-coarse sandy matrix with poorly sorted and sub-rounded pebbles (10%–20%). The pebbles ranged from 0.2 to 1.5 cm in size and displayed reverse-graded bedding (Fig. 3(b)). Further, scour surfaces, torn mud pebbles, and trough cross-beddings developed in the sandstones (Fig. 3(b) and S2(e)). The lonestone-bearing siltstone featured hugeness-thickness, parallel beddings, and normal-graded beddings (Figs. S6(a)–(b)). The lonestone-bearing mudstone contained heterolithic and poor-sorted dropstones ranging from 0.02–1.2 cm (Fig. 3(c)–(d) and S2(b)–(c)). Horizontal lamination often changed to draping laminations and impact structures due to glacial lonestones (Fig. 3(c)–(d) and S2(c)).

The upper transition strata were purplish-red, gray-green stratified sandstones interbedded with mudstones, siltstones, or limestone (Figs. 2, 3(f)–(j), S2(h), S3(a), and S8(a)). The sandstones were mainly lithic and composed of volcanic rock, mudstone, siltstone, quartz, and feldspar fragments with poorly sorted and sub-rounded features, and developed trough cross-beddings, scour surfaces, normal graded beddings, parallel beddings, horizontal beddings, swash cross-beddings, and ripple marks (Fig. 3(g)–(i), S3(c), and S7(b)–(c)). Notably, the cap dolomite (the C-E boundary marker layer) was missing in the study area.

4.2. LA-ICP-MS U–Pb dating of detrital zircons

Zircons preserved in the sandstone sample ZK117-1-49 were colorless with distinct oscillatory zoning under cathodoluminescence, which indicates a magmatic origin (Corfu et al., 2003). Cathodoluminescence images of representative zircons are presented in Fig. 4(a). They were euhedral to subhedral, with grain

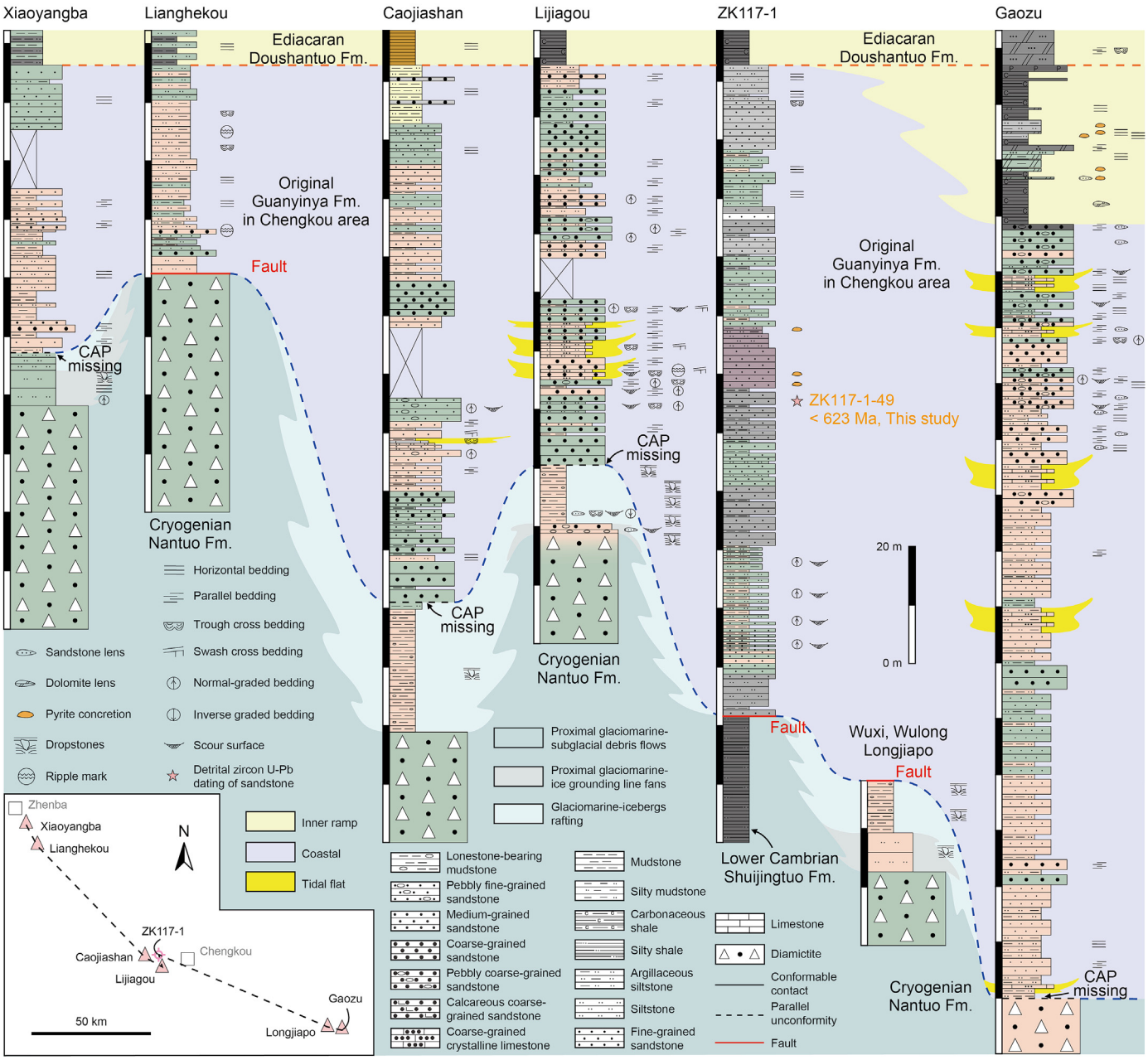

Fig. 2. Stratigraphic and sedimentary correlation of the Cryogenian-Ediacaran transition strata in the northeastern Sichuan Basin (NW-SE profile). CAP-Marinoan cap dolomite.

lengths ranging from 70 to 220 μm (most about 140 μm) and aspect ratios of 1:1 to 4:1. The euhedral grains indicated little or short-distance transport. In addition to oscillatory zoning, the Th/U ratios of the zircons ranged from 0.57 to 2.97, consistent with those of the magmatic origin (Belousova et al., 2002). A total of 100 analyses of 98 zircons were undertaken from sample ZK117-1-49. Most analyses were in the oscillatory zoning region of the zircon grains, with only a few analyses from the core of grains. Zircon U–Pb isotopic compositions are presented in Supplementary Data Table S1. Uncertainties in individual analyses in the data table and concordia plots are presented at 1 σ. All analyses are shown on concordia plots (Fig. 4(b)). However, analyses with greater than 10% discordance were not included in frequency diagrams (Fig. 4(c)), and ages less than 1000 Ma were based on the $^{206}Pb/^{238}U$ ratio, whereas older ages are based on the $^{206}Pb/^{207}Pb$ ratio. Ages calculated for multiple grains were quoted with a 95% confidence limits.

In sample ZK117-1-49, 84 of 100 analyses plotted on or near concordia and yielded ages ranging from 2.06–0.59 Ga. Age spectra were classified into three groups, with the oldest zircon yielding a $^{207}Pb/^{206}Pb$ age of 2063 ± 24 Ma, 91 analyses ranging from 666 to 588 Ma, and seven analyses ranging from 866 to 771 Ma. Two dominant peaks occurred at 622 Ma and 850 Ma (Fig. 4(c)), the ca. 622 Ma peak was produced by 84 zircon grain analyses which yielded a weighted mean $^{206}Pb/^{238}U$ age of 622 ± 2.4 Ma and a concordia age of 623 ± 2.7 Ma (Fig. 4(b)). The second age peaked at ca. 850 Ma, which was reproduced by six grain analyses.

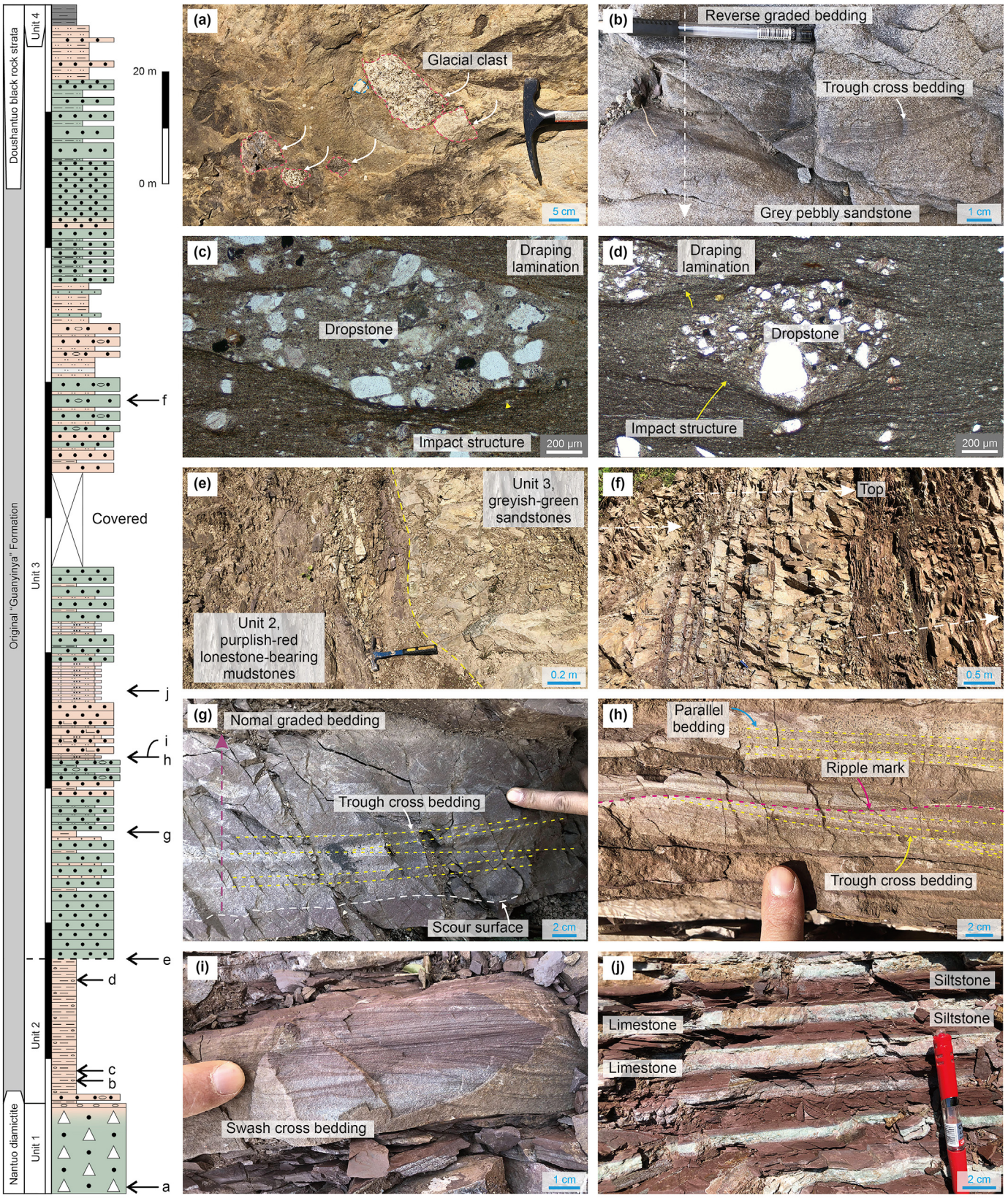
Doushantuo black rock strata
Unit 4
Unit 3
Unit 2
Unit 1
Original "Guanyinya" Formation
Nantuo diamictite
20 m
0 m
Covered
f
j
i
h
g
e
d
c
b
a
(a)
Glacial clast
5 cm
(b)
Reverse graded bedding
Trough cross bedding
Grey pebbly sandstone
1 cm
(c)
Draping lamination
Dropstone
Impact structure
200 μm
(d)
Draping lamination
Dropstone
Impact structure
200 μm
(e)
Unit 3, greyish-green sandstones
Unit 2, purplish-red lonestone-bearing mudstones
0.2 m
(f)
Top
0.5 m
(g)
Nomal graded bedding
Trough cross bedding
Scour surface
2 cm
(h)
Parallel bedding
Ripple mark
Trough cross bedding
2 cm
(i)
Swash cross bedding
1 cm
(j)
Siltstone
Siltstone
Limestone
Limestone
2 cm
Mudstone
Lonestone-bearing mudstone
Siltstone
Coarse-grained sandstone
Calcareous coarse-grained sandstone
Fine conglomerate
Silty mudstone
Argillaceous siltstone
Fine-grained sandstone
Pebbly coarse-grained sandstone
Coarse-grained crystalline limestone
Diamictite

5. Discussion

5.1. Stratigraphic correlation

5.1.1. Stratigraphic attribution of the original "Guanyinya Formation" in the Chengkou area

It was difficult to obtain precise and reliable depositional ages of the C-E siliciclastic rocks in the northeastern Sichuan Basin due to the absence of tuff. U–Pb ages of the youngest zircons constrain a maximum depositional age (Dickinson and Gehrels, 2009). The youngest group from the sandstone strata of the Chengkou "Guanyinya Formation" generated concordant ages ranging from 601 to 649 Ma (Table S1) with a concordia maximum deposition age of 623 ± 2.7 Ma (Fig. 4(c)). The youngest detrital zircon peak age of 622 Ma was obtained at the bottom of the DST in the adjacent Well WT-1 (He et al., 2021), and a tuff age of 633.4 ± 3.1 Ma above the DST I was reported in the Heyu section (Wang et al., 2020b). In South China, the tuff ages from the DST bottom, lower DST II, and middle DST II were 635.23 ± 0.57 Ma (Condon et al., 2005), 632.5 ± 0.48 Ma (Condon et al., 2005), and 614.0 ± 7.6 Ma (Liu et al., 2009), respectively. When combined with the above accurate tuff ages, this work suggested that the Chengkou "Guanyinya" sandstone strata accumulated in the early Ediacaran, approximately equivalent to DST II in South China (Fig. 2).

Previous studies generally concluded that the Chengkou "Guanyinya" sandstone strata directly overlaid the NT diamictites (Li and Zhou, 1995); however, 10–20 m of purplish-red, lonestone-bearing mudstone strata was observed between them (Figs. 2, 3(c)–(e), and S2(b)–(c)). The upward-fining glacial sequence at the top of the NT was the typical terminal deglacial sequence of the Marinoan Glaciation in South China (Jiang et al., 2011; Lang et al., 2018b; Chen et al., 2020). Thus, the lonestone-bearing mudstone strata were assigned to the Cryogenian. Notably, the cap dolomite was missing in the study area, while icebergs rafted lonestone at the bottom of the cap dolomite were reported in Namibia (Heron et al., 2020). However, this does not invalidate the above discussion as a drawdown in atmospheric pCO_2 levels after the intense chemical weathering and reverse weathering during the Marinoan terminal deglaciation period, likely led to the formation of the renewed glacier (Huang et al., 2016; Li et al., 2021a). Moreover, non-glacial marine facies clastic rock strata frequently developed at the top of the NT in South China (Jiang et al., 2011; Lang et al., 2018b; Chen et al., 2020), indicated that the Marinoan Glaciation melted earlier than the cap dolomite precipitation (Lang et al., 2018b).

In conclusion, based on the maximum depositional age and sedimentary sequence, the sandstone strata and the lonestone-bearing mudstone strata of the Chengkou "Guanyinya Formation" were assigned to the Ediacaran and the Cryogenian, respectively (Fig. 5). Similarly, the mudstone or sandstone strata overlying the NT glacial diamictites in northeastern Sichuan were sedimentary responses to the Cryogenian global terminal deglaciation (Fig. 2). The postglacial red sandstone strata presented consistent lithologic and sedimentary features throughout the northeastern Sichuan (Figs. 2 and 5); thus, they were all assigned to DST II.

5.1.2. Stratigraphic correlation framework

Analysis of the stratigraphy benefitted from the consistent stratigraphic features and sequence of the C-E transition strata along the NW-SE profile in the study area (Fig. 2). The Ediacaran red-green coastal sandstone strata were parallel unconformable overlaid the Cryogenian terminal deglacial clastic rock strata (Fig. 3(e), S3(a), and S6(c)), succeeded by the DST black rock strata and P–Mn-bearing strata (Figs. S3 and S5–7). The P–Mn deposits with a thickness of 2–15 m developed stably in the Zhenba-Chengkou area (Fig. S9), easily to recognized and marked the top DST boundary (Figs. S5 and S7(e); e.g., Zhang et al., 2021). This was supported by well-correlated chemostratigraphy of the Dengying Formation to the Three Gorges area (Chen et al., 2015) and the DST typical microfossils (Fig. S5), including *Archaeophycus yunnanensis* (Figs. S5(c)-(f)), *Megasphaera* (Zhang, 2014), and suspected *Wengania* (Fig. S5(b)).

The DST (ca. 90–154 m, without DST I cap dolomite) in the Zhenba-Chengkou area was divided into three lithostratigraphic members (Fig. 5): (i) DST II (48.5–110.0 m), a red and green sandstone strata with a maximum deposition age of 623 ± 2.7 Ma; (ii) DST III (29.0–59.0 m), a black mudstone strata; and (iii) DST IV (2.0–29.0 m), a phosphorous- or manganese-bearing strata. However, the DST in the Wuxi area displayed a transition feature to the eastern Shennongjia-Three Gorges area in stratigraphy, where the red coastal sandstone strata of the lower DST II had consistent sedimentary features with the northeastern Sichuan, and the upper DST II to DST IV was equivalent to the DST II–IV of the eastern Shennongjia-Three Gorges area (Fig. 5).

In conclusion, compared with the Ediacaran comprehensive stratigraphic framework of South China (Fig. 5; Zhou et al., 2019b, 2021 and references therein), the northeastern Sichuan DST was well correlated, and divisible into three members without the regional DST I cap dolomite. The Wuxi area is the transition region of the C-E transition strata along the northern Yangtze margin.

5.2. Sedimentary facies analysis

Based on stratigraphic thickness variations, the stacking pattern of lithofacies, and the lateral relationship between lithofacies, two typical depositional systems were recognized in the C-E transition strata of northeastern Sichuan, including glacial and barrier coastal-shelf systems (Nichol, 2009).

5.2.1. Glacial depositional system

5.2.1.1. Proximal glaciomarine environment. The proximal glaciomarine environments were dominated by massive diamictites (up to hectometers) in the study area, which were deposited explicitly from a series of subglacial debris flows (Allen et al., 2004), initiated in the ice margin zone, and accumulated structureless diamictite at the grounding line (Le Heron et al., 2013). Lenticular pebbly sandstones (Fig. S2(e)-–(g) and i) and massive lonestone-bearing siltstones (Fig. S6(a)) developed in Chengkou and Zhenba with parallel, cross, and graded beddings and scour surfaces (Figs. 3(b), S2(e), and S6(b)). This represented the debris flows deposits produced by the over-steepening of ice grounding line fans (Allen et al., 2004). The bounding surfaces of subglacial debris flows, and ice grounding line fans were typically planar with a steady distribution in transverse (Fig. 2); however, the latter changed rapidly in the branch flows. The massive lonestone-bearing siltstone differed

Fig. 3. Typical sedimentary rocks and structures of the Cryogenian-Ediacaran transition strata from the Lijiagou section, Chengkou area. **(a)** The massive greyish-green diamictites with glacial clasts; **(b)** The reverse graded bedding and trough cross-bedding in the pebbly sandstone lens; **(c), (d)** Completely isolated dropstones within the purplish-red mudstones show draping lamination and impact structure; **(e)** The Cryogenian-Ediacaran boundary shows the greyish-green stratified sandstones are parallel unconformably overlie the purplish-red lonestone-bearing laminated mudstones; **(f)** Upward-coarsening sequences show the sandstones gradually become thicker from bottom to top, while the mudstone layers become gradually thinner; **(g)** Sub-upward-fining sequence in single-bed sandstone show pebbly sandstones with scour surface and normal graded bedding in the bottom, and followed by sandstones with trough-cross bedding; **(h)** Trough cross-bedding, ripple marks, and parallel bedding; **(i)** Swash cross-bedding; **(j)** The thin-layer rhythmic of purplish-red siltstones and limestones.

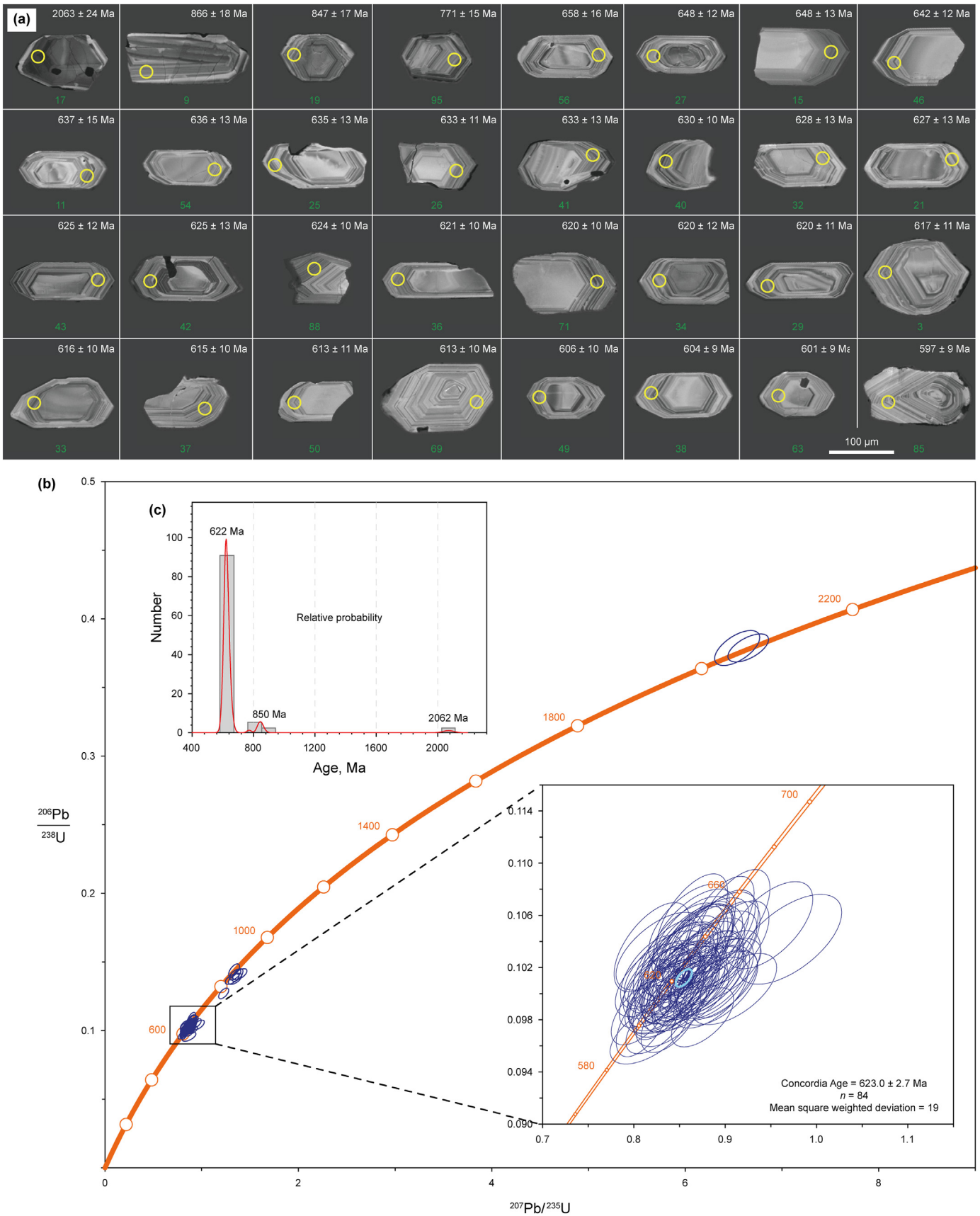

Fig. 4. Detrital zircon U–Pb dating results. **(a)** CL images of representative zircon grains. The yellow circles represent the sites of U–Pb age analyses; **(b)** U–Pb concordia diagram for siltstone detrital zircons of ZK117-1-49; **(c)** Normalized probability density distribution of the age data.

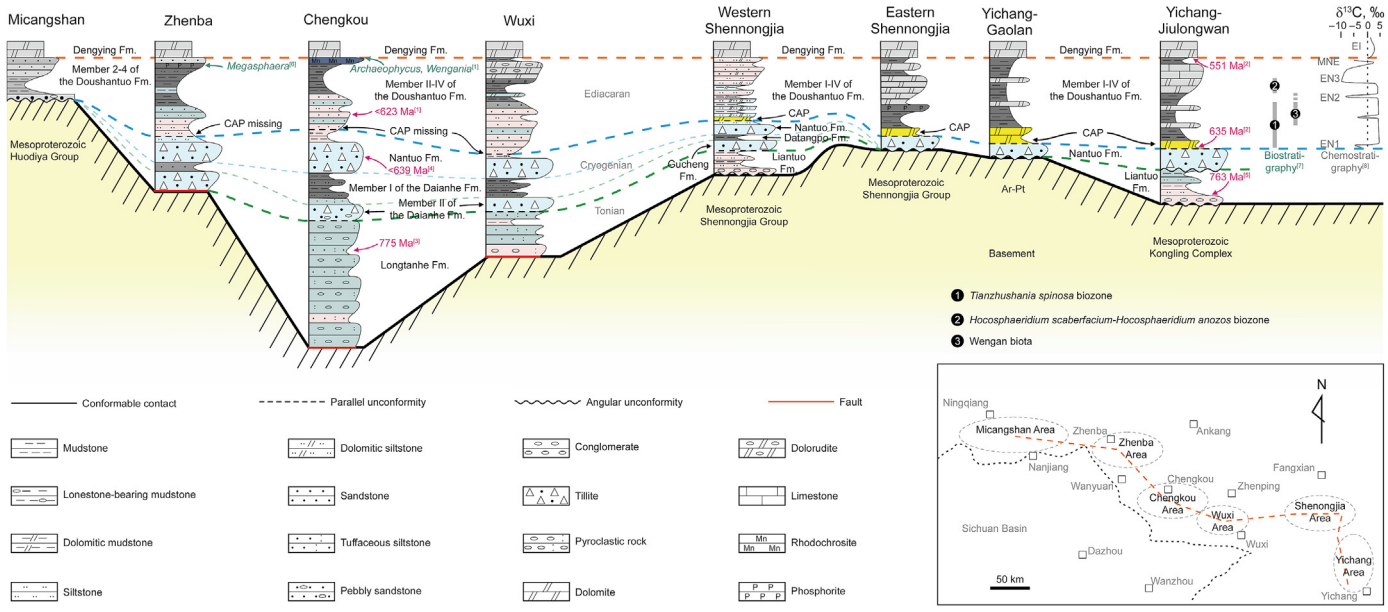

Fig. 5. The framework of stratigraphic subdivision and correlation for the Ediacaran Doushantuo Formation on the northern Yangtze margin (modified from Jiang et al., 2011; Wang et al., 2019; Li et al., 2021b; Kuang et al., 2022; Ye et al., 2022; Chen et al., 2023). The chronostratigraphy, biostratigraphy, and chemostratigraphy data are from: [1] This study; [2] Condon et al. (2005); [3] Xiang et al. (2015); [4] Huang et al. (2021); [5] Jing et al. (2018); [6] Zhang (2014); [7] Liu et al. (2016); and [8] Zhou et al. (2019b). CAP: Marinoan cap dolomite; EN: Ediacaran Negative $\delta^{13}C$ excursion; MNE: Miaohe $\delta^{13}C$ Negative Excursion; EI: Ediacaran Intermediate values. Note that there is no exact vertical scale, but a relative difference in thickness between each area, which enlarged the Ediacaran Doushantuo Formation.

from the distal glaciomarine lonestone-bearing sandstone, which was commonly thin-layered (Lang et al., 2018b).

5.2.1.2. Distal glaciomarine environment. Lonestone-bearing sandstones dominated the distal glaciomarine environments in the study area (Figs. 3(c)–d and S2(b)–(c)), and the bounding surfaces were typically planar with a steady distribution in transverse (Fig. 2). As the ice melted, abundant clastic materials rafted by icebergs were deposited in the glaciomarine environment, forming the lonestones (Le Heron, 2015).

5.2.1.3. Non-glacial slope environment. The gray-green mudstones were observed at the top of the NT in the Heyu section with clear features of pyrite concretions or beds within the mudstones (Fig. S4(b)). In South China, both sizes and abundance of pyrite concretions at the top of the NT displayed depth gradients, indicating a euxinic slope-basin environment (Lang et al., 2018a).

5.2.2. Barrier coastal-shelf depositional system

5.2.2.1. Coastal environment. The postglacial clastic rock strata in the study were characterized by sandstones interbedded with mudstones or siltstones (Figs. 3(f), S2(h), and S8(a)). The lithic sandstones had poorly sorted and sub-rounded features, suggesting a near-provenance and rapid accumulation process (Zhang et al., 2021). Typical sedimentary textures such as swash cross-beddings and ripple marks in sandstones (Figs. 3(g)–(i), S3(c), and S7(b)–(c)) indicated that these sediments formed above fair-weather wave bases where higher energy conditions from wave and longshore currents reworked the sediments (Nichol, 2009). Thus, a coastal environment was identified where the backshore, foreshore, and shoreface facies were distinguished by pebbly coarse sandstone, sandstone with swash cross-beddings or ripple marks, and siltstone, respectively. The tidal flat was dominated by thin interbedding of siltstones and limestones or dolomites (Figs. 3(j), S2(i), and S6(d)) with horizontal and minor cross-bedding (Fig. S3(d)). Moreover, frequent upward-coarsening successions represent the progradation of the beach to the shoreface (Fig. S9; Clifton, 2006). The bounding surfaces of coastal sandstones were typically planar with a steady distribution in transverse (Fig. 2).

5.2.2.2. Shelf environment (mixed carbonate-siliciclastic ramp). Based on the stratigraphic-sedimentary correlation and basin analysis, the shelf environment was recognized in Well WT-1 (Wang et al., 2021b), characterized by mudstone interbedded with sandstone and siltstones (He et al., 2021). The alternating mud and sand suggested alternating fair weather and storm sediments in the inner shelf environments (Nichol, 2009). Occasionally developed dolomites and microbialites suggested a mixed sedimentary environment. Similarly, a mixed carbonate-siliciclastic ramp depositional system was identified in the upper DST (Zhang et al., 2021), characterized by mixed deposition of mudstone, siltstone, dolomite, dolorudite, Mn-carbonate microbialites, and intraclast phosphorites (Figs. S3, S5, and S7(e)). A basin environment was identified at the upper DST at the Heyu section, dominated by black shales and siliceous rock (Wang et al., 2020b), suggesting that the ramp was distally steepening.

5.2.3. Vertical and lateral distributions of facies associations

5.2.3.1. Typical sedimentary sequence. The Lijiagou section was the most typical profile of the C-E transition strata in northeastern Sichuan, where glacial and barrier coastal depositional systems developed in the lower and upper strata, respectively (Fig. S10). The proximal and distal glaciomarine environments were identified in the glacial depositional system, the former consisting of subglacial debris flows and ice grounding line fans, and the latter consisting of icebergs rafting glaciomarine. Specifically, an upward-fining glacial sequence developed in the lower C-E transition strata, where massive glacial diamictites were followed by ice grounding line fans sandstones and icebergs rafting mudstones (Fig. S10), demonstrating a rapid sea level rise in response to global deglaciation.

Backshore, foreshore, shoreface, and tidal flat environments

were recognized in the upper coastal sandstone strata (Fig. S10). The upward-coarsening sequences were frequently developed, demonstrating that the sandstone became progressively thicker while the mudstone gradually became thinner (Fig. 3(f)), indicating a transformation from tidal flat to backshore or shoreface to foreshore (Fig. S10). Contrastingly, the upward-fining sequences only developed at the bottom and top, which demonstrated that the mudstone became progressively thicker while the sandstone gradually became thinner (Fig. S3(h)), indicating a transformation from foreshore to shoreface (Fig. S10). The sub-upward-fining sequence was typical in single-bed sandstone, pebbly sandstone with a scour surface developed at the bottom, followed by a decrease in pebble content (Fig. 3(g)). Thus, the regional sea level slightly fluctuated during the sedimentary period of the coastal sandstone strata.

In conclusion, the C-E transition strata in the study area showed a typical sedimentary sequence of a transition from distal glaciomarine diamictites to proximal glaciomarine lonestone-bearing mudstones, followed by coastal stratified lithic sandstones. This suggested a rapid sea level rise in response to deglaciation, followed by rapid regional sea level decline and maintenance of a relatively stable state.

5.2.3.2. Lateral variations in facies association. Along the NW-SE profile of the northeastern Sichuan Basin, similar vertical distributions of facies associations were identified in Zhenba, Chengkou, and Wuxi. The glacial depositional system with typical deglacial sequences, developed in the lower C-E transition strata and coastal sandstone strata set in the upper (Fig. 2). Specifically, the glacial deposits were missing in the Micangshan-Hannan ancient land and the coastal sandstones were thinner than 4.0 m (Wang et al., 2019). The Zhenba area was relatively close to the ancient land and dominated by the features of a proximal glaciomarine environment, such as ice grounding line fans consisting of deposited massive lonestone-bearing siltstone with parallel beddings (Fig. 2). The Chengkou-Wuxi area mainly developed the distal glaciomarine environment, where lonestone-bearing mudstones were deposited (Fig. 2). Along the profile of Micangshan-Zhenba-Chengkou-Wuxi, the occurrence of coastal sandstone strata gradually thickened (Fig. 2). In addition, mudstone and dolomite strata of the inner ramp overlaid the coastal sandstone strata in Wuxi (Fig. 2).

Along the SW-NE profile across the Sichuan Basin, the glacial strata were missing in the ancient land (Wang et al., 2019). The glacial depositional system with a typical deglacial sequence developed in northeastern Sichuan and south Qinling (Fig. S11). From the slope to the basin, the proximal glaciomarine lonestone-bearing mudstones developed in the Chengkou area and non-glacial marine mudstone with pyrite beds developed in South Qinling (Fig. S11). For the upper C-E transition strata, coastal clastic rocks wildly developed in western-central-northeastern Sichuan, gradually becoming thicker from the ancient land to the east or west (Fig. S11). In addition, the Kaijiang area developed shallow water shelf fine-grained clastic rocks with the largest thickness (> 250 m) of the study area (Fig. S11). A carbonate inner ramp developed in the South Qinling region, which was dominated by dolomites, showing a transition from shallow to relatively deep environments (Fig. S11).

In conclusion, the C-E transition strata display similar vertical stacking patterns in the study area and pronounced variations in facies association vertically and laterally. The stratum thickness and sedimentary environment clearly changed from the land to shallow sea, slope (shelf), and basin environment, probably due to the influence of the paleogeographic pattern during this period.

5.3. Sedimentary evolution and paleogeography during the Cryogenian-Ediacaran transition

5.3.1. Sedimentary provenance

The clastic composition is the most direct indicator of the rock types in the source areas, and their relative content differences can help in analyzing the provenance. The C-E transition strata in the study area contain many volcanic rock fragments (Figs. S2(d) and S12), which can also help analyze the provenance. A similar characteristic of volcanic fragments was recorded at the top of the NT and the DST II, mainly andesites, granites, basalts, and rhyolites (Figs. S2d, S8(c), and S12), suggesting that the early Ediacaran in the northeastern Sichuan probably succeeded the provenance of the late Cryogenian, both from the igneous rock zone of the surrounding areas (Fig. S9).

The age information recorded in detrital zircons can indirectly indicate the provenance of clastic rocks and assist in regional correlation and paleogeographic reconstruction. For DST II, the detrital zircon ages ranged from 665 to 588 Ma (peak age 622 Ma) and 865–771 Ma (peaks age 850 Ma) in Well ZK117-1 (Fig. 4(c) and 6(a)). Three age intervals (915–850, 794–714.5, and 700–622 Ma) with several peak ages were recorded in the adjacent Well WT-1 (Fig. 6(b); He et al., 2021). Notably, the detrital zircon age intervals of the DST II and the upper Cryogenian Nantuo (Muzuo) Formation in the northeastern Sichuan overlapped at 900–700 Ma for a large proportion (Fig. 6(c)), indicating that they likely have similar provenances. These peak ages were comparable with the numerous 900–700 Ma igneous bodies of the Micangshan-Hannan ancient land (Figs. 6 and S9; Huang et al., 2021 and references therein) and the basement of the Sichuan ancient land (Gu et al., 2015). It is supported by the zircons Lu–Hf isotopes data from the upper NT in the study area, which indicates the provenance was primarily from the northern Yangtze Block (Huang et al., 2021).

In conclusion, the clastic analysis and detrital zircon information indicated that the massive terrigenous clasts observed in the C-E transition strata in northeastern Sichuan mainly originated from the igneous zones of the Sichuan and Micangshan-Hannan ancient lands. The early Ediacaran in the study area succeeded the provenance of the late Cryogenian, which indicated that the paleogeographic pattern of the northern Yangtze margin was unlikely to have changed dramatically during the C-E transition.

5.3.2. Sedimentary evolution

5.3.2.1. Marinoan terminal deglaciation and glaciomarine sedimentary stage. At the end of the Cryogenian, a comprehensive factor, such as volcanism, induced the end of the Marinoan glaciation (Lan et al., 2022), and global deglaciation occurred. During this transition, the Sichuan and Micangshan ancient lands were glacially covered denudation zones (Fig. 7(a)–(b)), which continued to supply terrigenous detritus to the northeastern Sichuan region (He et al., 2021; Huang et al., 2021). However, the ice sheets in the study area gradually retreated in extent toward the Central Sichuan and the Micangshan-Hannan ancient lands. The retreating ice-sheet could have led to a significant sea-level rise and transformation of the glacial ice sheet to distal glaciomarine environments, resulting in an upward-fining sequence (Figs. 2 and S10). Typically, the proximal glaciomarine, distal glaciomarine, and non-glacial environments successively developed from shelf to slope (Figs. 2 and 7(b), and S11). Notably, massive non-glacial siltstone and mudstones indicated that some marine areas likely remained ice-free before the final melting stages of the Marinoan Glaciation (Lang et al., 2018a).

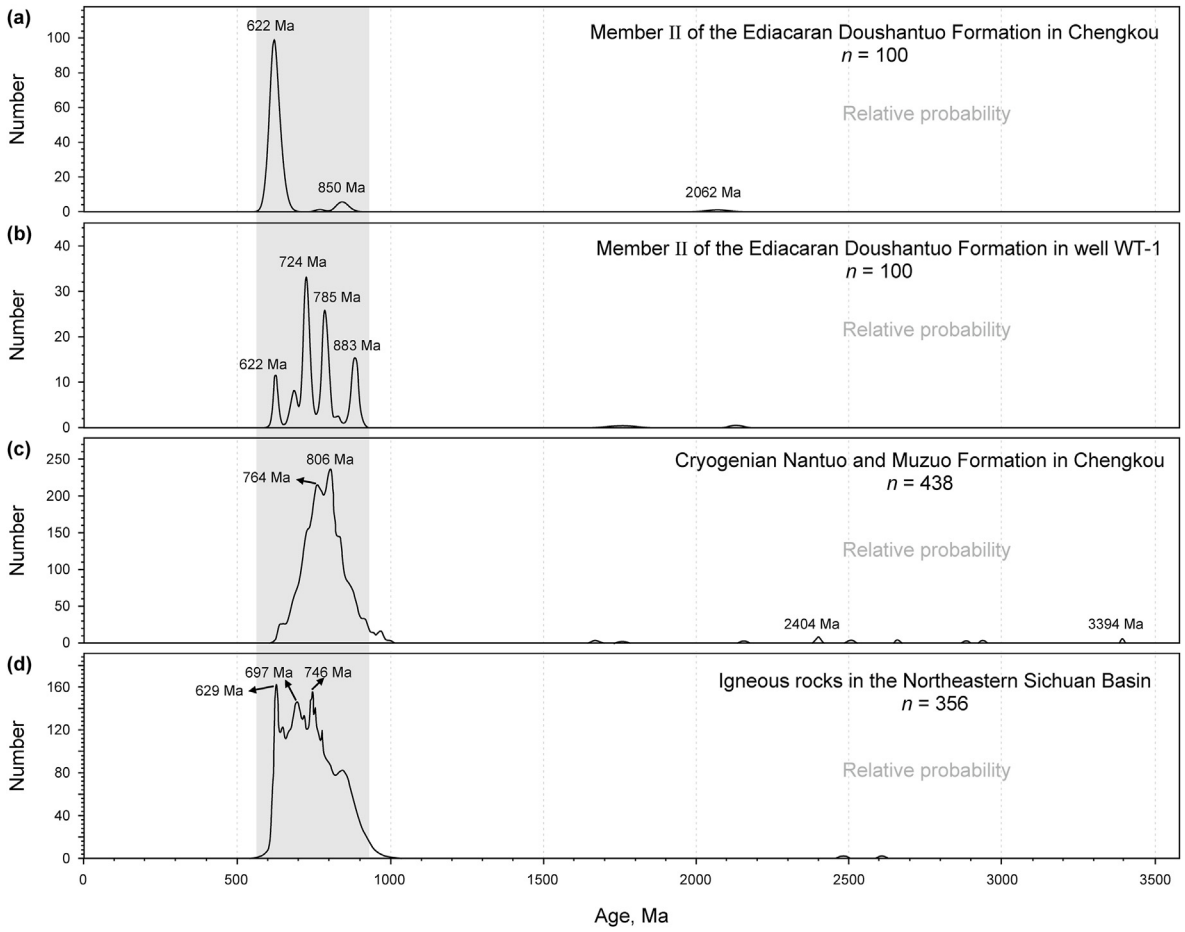

Fig. 6. Zircon U–Pb age probability curves of the Neoproterozoic sedimentary rocks and igneous rocks from the northeastern Sichuan Basin. Data sources: (b) He et al. (2021); (c), (d) Huang et al. (2021) and references therein.

5.3.2.2. Early Ediacaran filling-leveling up and coastal sedimentary stage. After the Marinoan Glaciation ended, the DST began depositing (Huang et al., 2016; Lang et al., 2018a), and the entire Yangtze Block entered a relatively stable development stage (Yang et al., 2020). The Sichuan Basin and the surrounding area succeeded the paleogeographic pattern of the terminal Cryogenian during the early Ediacaran. The Sichuan and Micangshan ancient lands continued to supply terrigenous clasts to the study area (Fig. 7(c)). Controlled by ancient lands and abundant terrestrial input, the study area was dominated by barrier coastal environments with near-source clastic rocks during this period (Fig. 7(c)). As the glacially eroded landforms were widely developed (Xiao et al., 2020), the topographic height difference of sedimentary areas led to the rapid changing of the stratigraphic lateral thickness (Fig. 2). However, the sandstone strata of the DST II filled the sub-depressions, even the Kaijiang area (> 250 m), and the whole study area changed into an inner ramp system in middle Ediacaran (Figs. 2 and S11).

5.4. Why the Marinoan cap dolomite missing in the northeastern Sichuan Basin

The Marinoan cap dolomite, as the C-E boundary marker layer, unconformably overlies the NT and records the first Ediacaran global negative $\delta^{13}C_{carb}$ event (Jiang et al., 2011). Marinoan cap dolomites were 0.4–10.0 m thick in the Yangtze region and typically had an abundant sedimentary structure such as sheet cracks, cavities, "tepee-like" structures, barite fans, low angle cross-bedding, stromatolites, giant ripple, and isopachous cemented brecciations (Ning et al., 2021). Along the profile of the western Shennongjia-eastern Shennongjia-Three Gorges, the closer to the ancient uplands (western Shennongjia), the thinner the cap dolomite thickness without the typical sedimentary structures and the stronger the bottom is diachronous (Fig. 5; Kuang et al., 2022). Although the cap dolomite was an extensive cap rock that gradually expanded from the marine to land environments, it responded favorably to the global transgression during the initial Ediacaran, resulting in diachronous control by the paleogeographic pattern.

CAP dolomite was not observed to overlay the NT in northeastern Sichuan (Fig. 2), except in the Heyu section in South Qinling (Fig. S4(b)). Moreover, the Marinoan cap dolomite layer was missing in the western-central-northern Sichuan Basin and eastern Yunnan (Figs. 2 and S11; Wang et al., 2019; Zhou et al., 2019a, 2021), where the Huize, Tianquan, Sichuan, and Micangshan-Hannan ancient lands were stable in the early Ediacaran (Wang et al., 2019). In the Eshan section, eastern Yunan, discontinuous dolostone nodules developed at the bottom of the Ediacaran, however, whether it belongs to the cap dolomite layer remains controversial (Zhou et al., 2021).

Along the NW-SE profile of the northern Yangtze margin (Fig. 5), sedimentological correlations show that cap dolomite developed in the carbonate ramp system of the Shennongjia-Three Gorges area (Kuang et al., 2022). In the west of Shennongjia, the lower DST consisted of near-source coastal clastic rocks without the cap

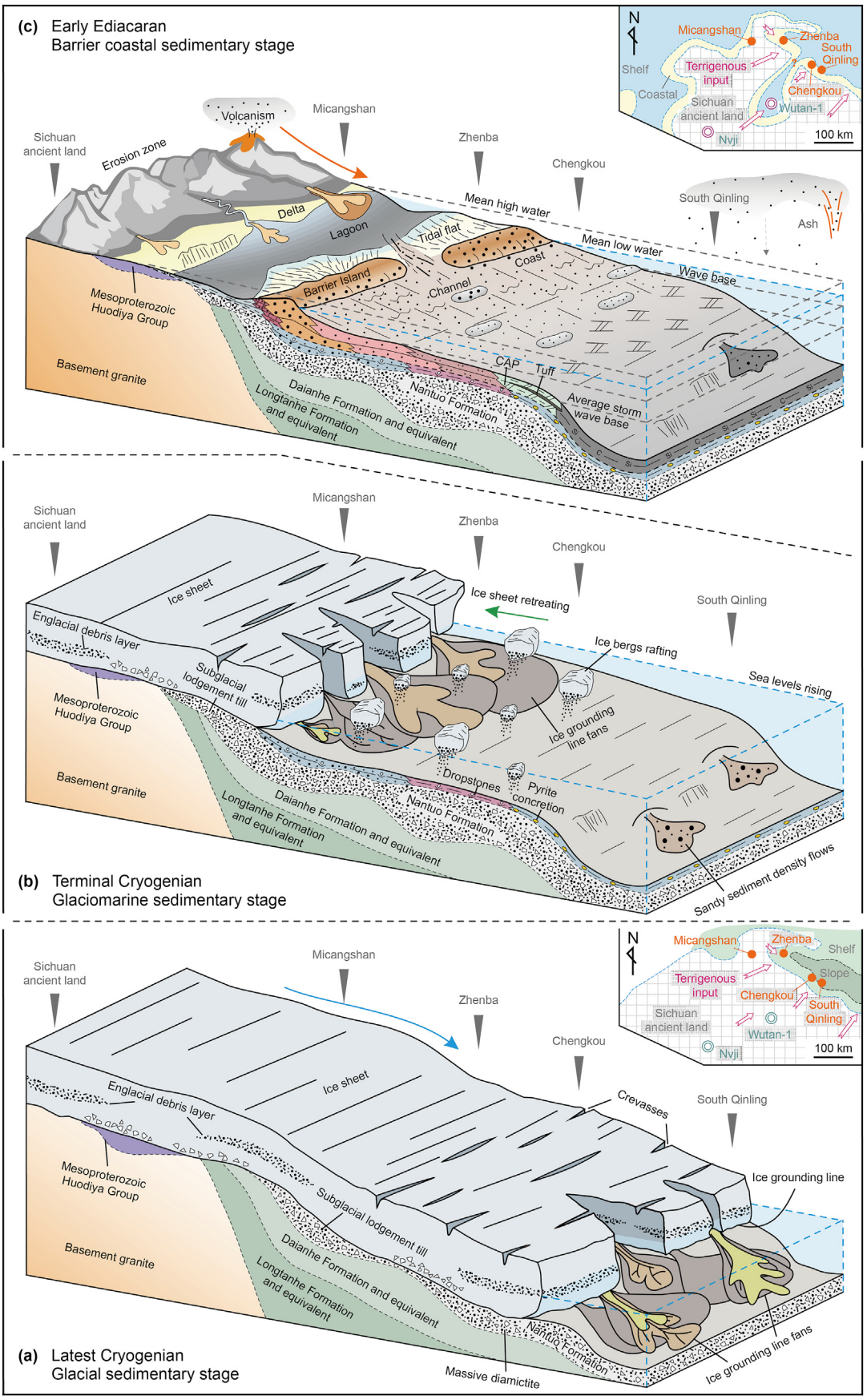

Fig. 7. Schematic diagram of sedimentary-tectonic evolution model for the Cryogenian-Ediacaran transition in northeastern Sichuan Basin, South China. CAP: Marinoan cap dolomite.

dolomite layer (Fig. 5). The sedimentary characteristics of the lower DST in Wuxi and western Shennongjia indicated that there was a coastal-ramp system transition region in the northern Yangtze Margin during this period (Fig. 5), similar to the transition from the northeastern Sichuan to south Qinling (Fig. S11). Furthermore, the stratigraphic and paleogeographic studies confirmed that stable ancient lands developed in all the above areas where the cap dolomite layer was absent (Wang et al., 2019), and the lower DST were all characterized by coastal clastic rocks (Figs. 5 and S11; Wang et al., 2019; Zhou et al., 2019a). Therefore, the ancient land and its large-scale terrestrial clast supply controlled the sedimentary system development, and the sedimentary system transformation likely explains the missing cap dolomite layer.

In conclusion, the sedimentary characteristics and thickness of the cap dolomite changed regularly due to its diachronous feature and the control of the paleogeographic pattern. The environment in the study area was unsuitable for carbonate deposition due to the control of the near ancient lands and the strong intervention of terrestrial detrital. Thus, the cap dolomite layer was missing.

5.5. Implications for hydrocarbon exploration

The new C-E stratigraphic framework of the northeastern Sichuan Basin drove us to re-examine the paleogeographic patterns during the middle to late Ediacaran Doushantuo period. The sedimentary and stratigraphic correlation showed that the black mudstone strata developed stably after the early Ediacaran filling-leveling up stage (Fig. 5). This indicated that the DST black shales with high TOC content (up to 17.9%, Zhu et al., 2022) and considerable thickness were deposited under a stable paleogeographic pattern (Zhang et al., 2021). The relatively stable paleogeographic pattern benefited from a favorable tectonic setting and reservoir-forming conditions. Thus, the Ediacaran System in the northeastern Sichuan Basin should be given high priority, especially the Doushantuo and Dengying source-reservoir-cap rocks combination, to realize large-scale, efficient exploration (Liu et al., 2019; Yang et al., 2022).

6. Conclusions

i) The late Cryogenian in northeastern Sichuan is characterized by 10–20 m of red glaciomarine lonestone-bearing mudstones as a sedimentary response to the Marinoan terminal deglaciation. The DST II is a 50–160 m red and green coastal sandstone strata with a 623 ± 2.3 Ma maximum depositional age, limited by detrital zircon U–Pb dating. Based on stratigraphic correlation in the study area and the Three Gorges area, the Marinoan cap dolomite is missing in northeastern Sichuan. The DST is proposed to be divided into three lithostratigraphic members without the regional Member I cap dolomite: (i) DST II red and green sandstone strata; (ii) DST III black mudstone strata; and (iii) DST IV P–Mn bearing strata.

ii) The C-E transition strata comprises glacial and barrier coastal-shelf depositional systems, the former including proximal glaciomarine, distal glaciomarine, and non-glacial slope facies, and the latter including backshore, foreshore, shoreface, and shelf (ramp) facies. In terms of stratigraphy, the upper NT proximal glaciomarine diamictites transitioned to the distal glaciomarine lonestone-bearing mudstones at the top and then changed upward to the DST barrier coast sandstones.

iii) Consistent with the upper NT, the DST II provenance is mainly from the Sichuan and Micangshan-Hannan ancient lands, indicating that the early Ediacaran succeeded the paleogeographic features of the late Cryogenian. Controlled by the ancient lands and glacially eroded landforms, the DST II is distinguished by barrier coast clastic rocks with a filling-leveling up feature. For the cap dolomite, the intense input of terrigenous clast, controlled by the paleogeographic pattern and its diachronous features, caused it to be missing in the study area.

Declaration of competing interest

The authors declare the following financial interests/personal relationships which may be considered as potential competing interests: Hongwei Kuang reports financial support was provided by China Geological Survey. Zhiwei Liao reports financial support was provided by National Natural Science Foundation of China. Zhiwei Liao reports financial support was provided by Chongqing Research Program of Basic Research and Frontier Technology. Zhiwei Liao reports was provided by Key Laboratory of Deep-time Geography and Environment Reconstruction and Applications of Ministry of Natural Resources, Chengdu University of Technology.

Acknowledgements

We appreciate the four anonymous reviewers for their insightful and constructive comments that greatly improved the quality of the manuscript. This study is supported by the China Geological Survey project (DD20221649), the National Natural Science Foundation of China (Nos. U19B6003, 42072135, and 42172119), Chongqing Research Program of Basic Research and Frontier Technology (Grant No. cstc2021jcyj-msxmX0023), and Open Fund (DGERA 20211105) of Key Laboratory of Deep-time Geography and Environment Reconstruction and Applications of Ministry of Natural Resources, Chengdu University of Technology.

Abbreviations

C-E: Cryogenian-Ediacaran; DST: Ediacaran Doushantuo Formation; DST I: Member I of the Doushantuo Formation; DST II: Member II of the Doushantuo Formation; DST III: Member III of the Doushantuo Formation; DST IV: Member IV of the Doushantuo Formation; NT: Cryogenian Nantuo Formation; CAP: Marinoan cap dolomite.

Appendix A. Supplementary data

Supplementary data to this article can be found online at https://doi.org/10.1016/j.petsci.2023.12.011.

References

Allen, P.A., Leather, J., Brasier, M.D., 2004. The Neoproterozoic Fiq glaciation and its aftermath, Huqf supergroup of Oman. Basin Res. 16, 507–534. https://doi.org/10.1111/j.1365-2117.2004.00249.x.

Belousova, E., Griffin, W., O'Reilly, S.Y., Fisher, N., 2002. Igneous zircon: trace element composition as an indicator of source rock type. Contrib. Mineral. Petrol. 143 (5), 602–622. https://doi.org/10.1007/s00410-002-0364-7.

Chen, X.S., Kuang, H.W., Liu, Y.Q., Wang, Y.C., Yang, Z.R., Vandyk, T.M., Heron, D.P.L., Wang, S.Y., Geng, Y.S., Bai, H.Q., Peng, N., Xia, X.X., 2020. Subglacial bedforms and landscapes formed by an ice sheet of Ediacaran–Cambrian age in west Henan, North China. Precambrian Res. 344, 105727. https://doi.org/10.1016/j.precamres.2020.105727.

Chen, X.S., Kuang, H.W., Liu, Y.Q., Heron, D.P.L., Wang, Y.C., Bai, H.Q., Peng, N., Xia, X.X., 2023. Sedimentology of the ediacaran barite-bearing cap dolostone from gaolan, northern three Gorges, south China. Sedimentology 70, 381–406. https://doi.org/10.1111/sed.13051.

Chen, Y.L., Chu, X.L., Zhang, X.L., Zhai, M.G., 2015. Carbon isotopes, sulfur isotopes, and trace elements of the dolomites from the Dengying Formation in Zhenba area, Southern Shaanxi: implications for shallow water redox conditions during the terminal Ediacaran. Sci. China Earth Sci. 58, 1107–1122. https://doi.org/10.1007/s11430-015-5071-0.

Clifton, H.E., 2006. A reexamination of facies models for clastic shorelines. In:

Posamentier, H.W., Walker, R.G. (Eds.), Facies Models Revisited, vol. 84. SEPM Special Publication, Tulsa, pp. 293–337.
Condon, D., Zhu, M.Y., Bowring, S., Wang, W., Yang, A.H., Jin, Y.G., 2005. U-Pb ages from the neoproterozoic Doushantuo Formation. Science 308 (5718), 95–98. https://doi.org/10.1126/science.1107765.
Corfu, F., Hanchar, J.M., Hoskin, P.W.O., Kinny, P., 2003. Atlas of zircon textures. Rev. Mineral. Geochem. 53, 469–495. https://doi.org/10.2113/0530469.
Dickinson, W.R., Gehrels, G.E., 2009. Use of U-Pb ages of detrital zircons to infer maximum depositional ages of strata: a test against a Colorado Plateau Mesozoic database. Earth Planet Sci. Lett. 288, 115–125. https://doi.org/10.1016/j.epsl.2009.09.013.
Gu, Z.D., Zhai, X.F., Yuan, M., 2015. Zircon U-Pb dating, geochemical characteristics and tectonic setting of basal granites in the Sichuan Basin. Acta Geol. Sin. 89 (Suppl. p), 296 (**in Chinese**).
He, Y., Wen, L., Luo, B., Zhou, G., Wang, Q.Y., Li, F.Y., Jia, M., Chen, Y.L., Bai, X.L., 2021. Source and tectonic background analysis of the sinian Doushantuo Formation in well WT 1 in Kaijiang area, Sichuan Basin. J. Palaeogeogr. 23 (4), 683–702 (**in Chinese**).
Heron, D.P.L., Busfield, M.E., Kettler, C., 2020. Ice-rafted dropstones in "postglacial" Cryogenian cap carbonates. Geology 49 (3), 263–267. https://doi.org/10.1130/G48208.1.
Hou, K.J., Li, Y.H., Tian, Y.Y., 2009. In situ U-Pb zircon dating using laser ablation-multiion counting-ICP-MS. Miner. Deposits 28, 481–492 (**in Chinese**).
Huang, H.Y., He, D.F., Li, D., Li, Y.Q., 2021. Zircon U-Pb ages and Hf isotope analysis of Neoproterozoic Yaolinghe Group sedimentary rocks in the Chengkou area, South Qinling: provenance and paleogeographic implications. Precambrian Res. 355 (7022), 106088. https://doi.org/10.1016/j.precamres.2020.106088.
Huang, K.J., Teng, F.Z., Shen, B., Xiao, S.H., Lang, X.G., Ma, H.R., Fu, Y., Peng, Y.B., 2016. Episode of intense chemical weathering during the termination of the 635 Ma Marinoan glaciation. Proc. Natl. Acad. Sci. U.S.A. 113 (52), 14904–14909. https://doi.org/10.1073/pnas.1607712113.
Jiang, G.Q., Shi, X.Y., Zhang, S.H., Wang, Y., Xiao, S.H., 2011. Stratigraphy and paleogeography of the ediacaran Doushantuo Formation (ca. 635–551Ma) in South China. Gondwana Res. 19 (4), 831–849. https://doi.org/10.1016/j.gr.2011.01.006.
Jing, X.Q., Yang, Z.Y., Tong, Y.B., Wang, H., Xu, Y.C., 2018. A SHRIMP U-Pb zircon geochronology of a tuff bed from the bottom of Liantuo Formation in the Three Gorges area and its geological implications. J. Jilin Univ. 48 (1), 165–180 (In Chinese).
Kuang, H.W., Liu, Y.Q., Peng, N., Vandyk, T.M., Heron, D.P.L., Zhu, Z.C., Bai, H.Q., Wang, Y.C., Wang, Z.X., Zhong, Q., Chen, J.X., Yu, H.L., Chen, X.S., Song, C.G., Qi, K.N., 2022. Ediacaran cap dolomite of Shennongjia, northern Yangtze craton, south China. Precambrian Res. 368, 106483. https://doi.org/10.1016/j.precamres.2021.106483.
Lan, Z.W., Huyskens, M.H., Le Hir, G., Mitchell, R.N., Yin, Q.Z., Zhang, G.Y., Li, X.H., 2022. Massive volcanism may have foreshortened the Marinoan snowball earth. Geophys. Res. Lett. 49, e2021GL097156. https://doi.org/10.1029/2021GL097156.
Lang, X.G., Shen, B., Peng, Y.B., Xiao, S.H., Zhou, C.M., Bao, H.M., Kaufman, A.J., Huang, K.J., Crockford, P.W., Liu, Y.G., Tang, W.B., Ma, H.R., 2018a. Transient marine euxinia at the end of the terminal Cryogenian glaciation. Nat. Commun. 9 (1), 3019. https://doi.org/10.1038/s41467-018-05423-x.
Lang, X.G., Chen, J.T., Cui, H., Man, L., Huang, K.J., Fu, Y., Zhou, C.M., Shen, B., 2018b. Cyclic cold climate during the Nantuo glaciation: evidence from the cryogenian Nantuo Formation in the Yangtze block, south China. Precambrian Res. 310. https://doi.org/10.1016/j.precamres.2018.03.004, 243–25.
Le Heron, D.P., 2015. The significance of ice-rafted debris in Sturtian glacial successions. Sediment. Geol. 322, 19–33. https://doi.org/10.1016/j.sedgeo.2015.04.001.
Le Heron, D.P., Busfield, M.E., Kamona, F., 2013. An interglacial on snowball earth? Dynamic ice behaviour revealed in the Chuos Formation, Namibia. Sedimentology 60 (2), 411–427. https://doi.org/10.1111/j.1365-3091.2012.01346.x.
Li, F.B., Penman, D., Planavsky, N., Knudsen, A., Zhao, M.Y., Wang, X.L., Isson, T., Huang, K.J., Wei, G.Y., Zhang, S., Shen, J., Zhu, X.K., Shen, B., 2021a. Reverse weathering may amplify post-Snowball atmospheric carbon dioxide levels. Precambrian Res. 364, 1–12. https://doi.org/10.1016/j.precamres.2021.106279.
Li, Z.W., Ran, B., Xiao, B., Song, J.M., Zheng, L., Li, J.X., Xiao, B., Ye, Y.H., Cai, Q.X., Liu, S.G., 2019. Sinian to early Cambrian uplift-depression framework along the northern margin of the Sichuan Basin, Central China and its implication for hydrocarbon exploration. Earth Sci. Front. 26 (1), 59–85 (in Chinese).
Li, L.S., Wang, Z.C., Xiao, A.C., Yang, G.Y., Jiang, H., Su, N., Wu, L., Shi, P.P., Wang, Y.P., 2021b. The rift system in northern Yangtze block during the Nanhua period: implications from gravity anomaly and sedimentology. Earth Sci. 46 (10), 3496–3508 (In Chinese).
Li, Z.H., Zhou, D.Y., 1995. The People's Republic of China, 1:5w Regional Geological Survey Report of Chengkou Mappable Unit (H-49-2-A). Geological Team of Southeastern Sichuan, Sichuan Bureau of Geology and Mineral Resources, Chongqing, pp. 1–20 (in Chinese).
Liu, P.J., Yin, C.Y., Gao, L.Z., Tang, F., Chen, S.M., 2009. New material of microfossils from the ediacaran Doushantuo Formation in the zhangcunping area, Yichang, Hubei province and its zircon SHRIMP U-Pb age. Chin. Sci. Bull. 54 (6), 1058–1064. https://doi.org/10.1007/s11434-008-0589-6.
Liu, P.J., Yin, C.Y., Tang, F., 2016. Progress in biostratigraphy of the ediacaran (sinian) of South China. In: Sun, S., Wang, T.G. (Eds.), Meso-Neoproterozoic Geology and Petroleum Resources in Eastern China. Science Press, Beijing, pp. 89–103 (in Chinese).
Liu, Q.Y., Zhu, D.Y., Jin, Z.J., Meng, Q.Q., Li, S.J., 2019. Influence of volcanic activities on redox chemistry changes linked to the enhancement of the ancient Sinian source rocks in the Yangtze Craton. Precambrian Res. 327, 1–13. https://doi.org/10.1016/j.precamres.2019.02.017.
Ludwig, K.R., 2003. User's Manual for Isoplot 3.00: A Geochronological Toolkit for Microsoft Excel, vol. 4. Berkeley Geochronological Center Special Publication, pp. 25–32.
Nichol, G., 2009. Sedimentology and Stratigraphy, second ed. Wiley-Blackwell, Oxford, pp. 1–419.
Ning, M., Yang, F., Ma, H.R., Lang, X.G., Shen, B., 2021. Precipitation of Marinoan cap carbonate from Mn-enriched seawater. Earth Sci. Rev. 218, 103666. https://doi.org/10.1016/j.earscirev.2021.103666.
Norris, A., Danyushevsky, L., 2018. Towards Estimating the Complete Uncertainty Budget of Quantified Results Measured by LA-ICP-MS. Goldschmidt, Boston, 2018-08-12.
Wang, H., Li, Z.W., Liu, S.G., Ran, B., Song, J.M., Li, J.X., Ye, Y.H., Li, N., 2020a. Ediacaran extension along the northern margin of the Yangtze platform, south China: constraints from the lithofacies and geochemistry of the Doushantuo Formation. Mar. Petrol. Geol. 112, 104056. https://doi.org/10.1016/j.marpetgeo.2019.104056.
Wang, H., Wu, W.H., Liu, S.G., Zhang, X.H., Song, J.M., Li, S.J., Ran, B., Wang, Z.J., Han, Y.Y., Wang, W.D., Wang, Z., Li, Z.W., 2020b. Initial separation of the South Qinling terrane from the Yangtze block during the ediacaran: insights from sequence correlation and zircon Hf isotope of tuff. Mar. Petrol. Geol. 112, 104613. https://doi.org/10.1016/j.marpetgeo.2020.104613.
Wang, W., Zhai, M.G., Hu, P.Y., Chung, S.L., Tang, Y., Wang, H.T., Zhu, Z.C., Wu, H., Huang, Z.Q., 2021a. Simultaneous growth and reworking of the Lhasa basement: a case study from Early Cretaceous magmatism in the north-central Tibet. Lithos 380–381, 105863. https://doi.org/10.1016/j.lithos.2020.105863.
Wang, Z.C., Liu, J.J., Jiang, H., Huang, S.P., Wang, K., Xu, Z.Y., Jiang, Q.C., Shi, S.Y., Ren, M.Y., Wang, T.Y., 2019. Lithofacies paleogeography and exploration significance of Sinian Doushantuo depositional stage in the middle-upper Yangtze region, Sichuan Basin, SW China. Petrol. Explor. Dev. 46 (1), 41–53. https://doi.org/10.1016/S1876-3804(19)30004-7.
Wang, Z.J., Wang, Z.C., Yu, Q., Yang, F., 2021b. Reconfirmation of Neoproterozoic intra-cratonic rift in northeast Sichuan and its significance of deep oil and gas. Sediment. Geol. Tethyan Geol. 41 (3), 361–375 (in Chinese).
Xiang, Z.J., Yan, Q.R., White, J.D.L., Song, B., Wang, Z.Q., 2015. Geochemical constraints on the provenance and depositional setting of Neoproterozoic volcaniclastic rocks on the northern margin of the Yangtze block, China: implications for the tectonic evolution of the northern margin of the Yangtze Block. Precambrian Res. 264, 140–155. https://doi.org/10.1016/j.precamres.2015.04.012.
Xiao, D., Cao, J., Luo, B., Tan, X.C., Xiao, W.Y., He, Y., Li, K.Y., 2020. Neoproterozoic postglacial paleoenvironment and hydrocarbon potential: a review and new insights from the Doushantuo Formation Sichuan basin, China. Earth Sci. Rev. 212, 103453. https://doi.org/10.1016/j.earscirev.2020.103453.
Yang, F.L., Zhou, X.F., Peng, Y.X., Song, B.W., Kou, X.H., 2020. Evolution of Neoproterozoic basins within the Yangtze Craton and its significance for oil and gas exploration in South China: an overview. Precambrian Res. 337, 105563. https://doi.org/10.1016/j.precamres.2019.105563.
Ye, Q., Li, J.Q., Tong, J.N., An, Z.H., Hu, J., Xiao, S.H., 2022. A microfossil assemblage from the ediacaran Doushantuo Formation in the Shennongjia area (Hubei province, south China): filling critical paleoenvironmental and biostratigraphic gaps. Precambrian Res. 377, 106691. https://doi.org/10.1016/j.precamres.2022.106691.
Yang, Y., Wang, Z.C., Wen, L., 2022. Sinian hydrocarbon accumulation conditions and exploration potential at the northwest margin of the Yangtze region, China. Petrol. Explor. Dev. 49 (2), 272–284. https://doi.org/10.1016/S1876-3804(22)60023-5.
Zhang, J., 2015. Sequence Stratigraphy of the Doushantuo Formation and Mineralization of Manganese in Chengkou Area, Chongqing City. Master's Thesis. Chengdu University of Technology, Chengdu, pp. 1–55 (in Chinese).
Zhang, Y., Chen, L., Li, J., et al., 2021. Preliminary study of manganese carbonate microbialite sedimentary environment of the Doushantuo Formation in northeast Chongqing. Acta Sedimentol. Sin. 39 (6), 1387–1405 (in Chinese).
Zhang, Y., 2014. Investigation of phosphatized microfossils from the ediacaran Doushantuo Formation of the northern margin of the Yangtze plate, Zhenba, south shaanxi. Master's Thesis. Northwest University, Xi'an, pp. 1–67 (in Chinese).
Zhou, C.M., Huyskens, M.H., Lang, X.G., Xiao, S.H., Yin, Q.Z., 2019a. Calibrating the terminations of Cryogenian global glaciations. Geology 251, 251–254. https://doi.org/10.1130/G45719.1.
Zhou, C.M., Yuan, X.L., Xiao, S.H., Chen, Z., Hua, H., 2019b. Ediacaran integrative stratigraphy and timescale of China. Sci. China Earth Sci. 62, 7–24. https://doi.org/10.1007/s11430-017-9216-2.
Zhou, C.M., Ouyang, Q., Wang, W., Wan, B., Guan, C.G., Chen, Z., Yuan, X.L., 2021. Lithostratigraphic subdivision and correlation of the Ediacaran in China. J. Stratigr. 45 (3), 211–221 (in Chinese).
Zhu, D.Y., Liu, Q.Y., Wang, J.B., Hu, G., Ding, Q., 2022. Transition of seawater conditions favorable for development of microbial hydrocarbon source–Reservoir assemblage system in the Precambrian. Precambrian Res. 374, 106649. https://doi.org/10.1016/j.precamres.2022.106649.